Single- and double-photoionization cross sections of nitric oxide (NO) and ionic fragmentation of NO^+ and NO^{2+}

Toshio Masuoka
Department of Applied Physics, Osaka City University, Sumiyoshi-ku, Osaka 558, Japan
(Received 8 April 1993)

Single- and double-photoionization processes of gaseous nitric oxide (NO) have been studied in the photon energy region 37–100 eV by use of time-of-flight mass spectrometry and a photoion-photoion-coincidence method together with synchrotron radiation. The single- (σ^+) and double- (σ^{2+}) photoionization cross sections of NO are determined. Dissociation ratios of the precursors NO^+ and NO^{2+} are determined separately at the excitation energies where the single and double photoionization are in competition. The results show that the metastable NO^{2+} ions amount to about 15% at higher photon energies in the double-photoionization processes. Ionic branching ratios and the partial cross sections for the individual ions produced from the precursors NO^+ and NO^{2+} are also presented. The threshold for the dissociative double photoionization was found to be 41.0±0.5 eV.

PACS number(s): 33.80.Eh, 33.80.Gj

I. INTRODUCTION

In recent years, considerable attention has been directed to the diatomic molecular dications such as CO^{2+} and NO^{2+} [1,2] in the gaseous phase. Despite the Coulomb (electrostatic) repulsion between two positively charged atomic ions at large internuclear distances, these dications in low-lying electronic states are stable for at least a few microseconds due to the presence of attractive chemical forces at smaller internuclear distances. These metastable electronic states lie at about a few electron volts or more above the corresponding dissociation limits. When these neutral molecules AB are excited by sufficiently energetic photons or charged particles, however, the relative abundance of these metastable dications (CO^{2+} and NO^{2+}) observed in usual mass spectrometry has been reported to be very small [3–6]. This observation, when considered alone, may assign too much importance to the formation of AB^{2+}, because dissociation to A^+ plus B^+ at higher excitation energies is not properly taken into account. Therefore, the present study focuses on the determination of the partial cross sections for the single and double photoionization of nitric oxide at excitation energies where both processes take place concomitantly because the probability of two-electron ejection is important in the understanding of electron correlations.

In the present study, the time-of-flight (TOF) mass spectrometry and photoion-photoion coincidence (PIPICO) methods were used together with synchrotron radiation. It is necessary to use two such complementary experimental methods to determine the partial cross sections because TOF mass spectra provide only the ion branching ratios for the final ionic products originating from the precursors AB^+ and AB^{2+} in a μsec time scale and PIPICO spectra provide only the intensity of dissociation channel ($A^+ + B^+$) of AB^{2+}. The ratio of the dissociative to the nondissociative processes is usually unknown. Consequently, in order to determine the partial cross section for double photoionization (for molecules for which both dissociative and nondissociative processes of dications are in competition), a method to bridge the TOF and PIPICO spectra was recently developed and applied to carbonyl sulfide [7]. This method is applied to the molecular and dissociative single and double photoionization of nitric oxide in the present study. No absolute cross-section measurements have been reported for the molecular and dissociative single- and double-photoionization processes in NO prior to the present study. Ion branching ratios and the partial cross sections for the individual ions produced from the precursors NO^+ and NO^{2+} are also separately determined.

Previous investigations on NO^{2+} include photon and electron-impact ionization mass spectrometry [3–6], Auger spectroscopy [2,8], translational energy spectroscopy (TES) [9–12], double-charge-transfer spectroscopy (DCTS) [13,14], photoion-photon of fluorescence coincidence measurements (PIFCO) [15,16], coincidence measurements of cation pair (PIPICO for photoionization) [17,18], kinetic-energy-release measurements [19,20], observation of emission spectrum [21,22], and theoretical calculations [2,21,23–27]. An excellent review of theoretical and experimental work on NO^{2+} prior to 1986 can be found in Ref. [25]. Although the appearance potential of NO^{2+}, as described in the current literature, ranges from 35.1 to 39.8 eV [25], the closest approximation to date seems to be 38.6±0.1 eV [2,14,15]. The observation of two emissions ($B\,^2\Sigma^+ \rightarrow X\,^2\Sigma^+$ and $A\,^2\Pi^+ \rightarrow X\,^2\Sigma^+$) indicates that the $A\,^2\Pi$ and $B\,^2\Sigma^+$ states of NO^{2+} are quasibound states [15,16], despite some recent *ab initio* calculations [25] that do not support the bound nature of the $B\,^2\Sigma^+$ state.

II. EXPERIMENTAL PROCEDURE

The photoion branching ratios and photoion-photoion coincidence (PIPICO) spectra were measured with the use of a time-of-flight (TOF) mass spectrometer, the details of which have been described elsewhere [28,29]. A

typical TOF mass spectrum measured at $h\nu=80$ eV is shown in Fig. 1.

The TOF mass spectrometer could be rotated through 90° around the photon beam in order to measure angular distributions of photoions and/or photoelectrons. The TOF mass spectra and the PIPICO spectra were measured at an angle of ~55° with respect to the polarization vector where the second-order Legendre polynomial is zero. This setting minimizes any effects of anisotropic angular distributions of fragment ions. The total electron signals detected by the channel electron multiplier were fed into the start input of a time-to-amplitude converter (TAC) for the measurement of TOF mass spectra. Using this method, the relative ion yields are affected by the photoelectron's kinetic energies, and the fragment ions such as NO^{2+}, N^+, and O^+ produced in double photoionization at higher excitation energies are overestimated, whereas those produced in single photoionization are underestimated by TOF mass spectrometry. This discrimination effect against energetic photoelectrons will be mentioned later in more detail. The absolute collection efficiencies of energetic fragment ions in the TOF mass spectrometer calculated with a computer program indicate that no conditions exist under which all ion pairs are collected even if the total kinetic energy of the fragment ions is smaller than 1 eV (collection rate of 96%), and the rate of the fragment ions with a total kinetic energy of 20 eV is 80%.

The main chamber, including the TOF mass spectrometer and the ionization chamber, was evacuated to a pressure of 5×10^{-9} Torr. The sample gas pressure in the ionization chamber was not directly measured during the experiments and was maintained so as to keep the background pressure in the main chamber at about 5×10^{-7} Torr.

Monochromatic radiation was provided by a constant-deviation grazing incidence monochromator installed at the UVSOR (UltraViolet Synchrotron Orbital Radiation) facility in Okazaki and Al optical filters (two Al filters for 37–60 eV, one Al filter for 60–70 eV, no filter above 70 eV). The bandpass of the monochromator was about 0.8 Å with 200-μm-wide entrance and exit slits.

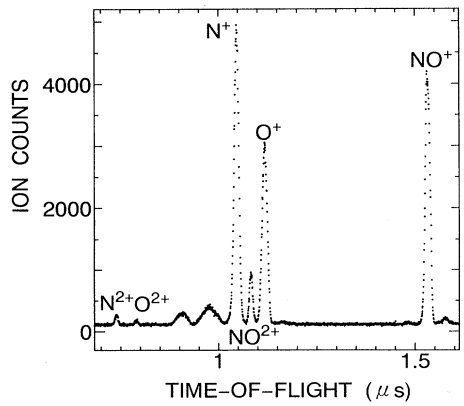

FIG. 1. Time-of-flight mass spectrum measured at a photon energy of 80 eV. The two broad humps between the O^{2+} and N^+ peaks occurring at higher photon energies are unidentified.

III. DATA ANALYSIS

The method used for the data analysis was described previously in the case of carbonyl sulfide [7]. In this case, the triple photoionization was observed in addition to the double photoionization, and the number of the dissociation channels of OCS^{2+} and OCS^{3+} was six. Therefore, the formulation of the method was rather complicated. For the diatomic molecule NO, the method for the data analysis is relatively simple.

A. Determination of the ion and electron detection efficiencies

Double photoionization takes place above 38.5 eV and is partially dissociative above 41.0 eV. These thresholds were obtained in the present study. The observed ions in the TOF mass spectra are NO^+, N^+, O^+, NO^{2+}, N^{2+}, and O^{2+} at excitation energies above 67.5 eV (Fig. 1). Triple photoionization was not observed.

Let N_s and N_d represent the rates of single and double photonionization, respectively, and ξ_s and $\xi_d+\zeta_d$ are the ratios of dissociative single and double photoionization, respectively. Then the overall scheme of photoionization is represented by

$$AB+h\nu \rightarrow AB^+(N_s) \rightarrow A_s^+, B_s^+ \quad (\xi_s), \tag{1a}$$

$$\rightarrow AB^+ \quad (1-\xi_s), \tag{1b}$$

$$\rightarrow AB^{2+}(N_d) \rightarrow A_d^+ + B_d^+ \quad (\xi_d), \tag{1c}$$

$$\rightarrow A^{2+}, B^{2+} \quad (\zeta_d), \tag{1d}$$

$$\rightarrow AB^{2+} \quad (1-\xi_d-\zeta_d)\,. \tag{1e}$$

The following four count rates experimentally measured in the mass and PIPICO modes, I (ion), E (electron), C_{IE} (electron-ion coincidence), and C_{II} (ion-ion coincidence), are given by

$$\mathrm{I}=f_i N_s+f_i(1+\xi_d)N_d\,, \tag{2}$$

$$\mathrm{E}=f_s N_s+f_d N_d\,, \tag{3}$$

$$C_{\mathrm{EI}}=f_i f_s N_s+f_i f_d(1+\xi_d)N_d\,, \tag{4}$$

$$C_{\mathrm{II}}=f_i^2\xi_d N_d\,, \tag{5}$$

where f_i is the ion detection efficiency (ion collection efficiency in the TOF plus detection efficiency), and f_s and f_d are the electron detection efficiencies for one- and two-electron ejections in the single and double photoionization, respectively.

In these equations, it is assumed that the ion detection efficiency f_i is the same for the different ionic species originating from single and double photoionization and does not depend on the excitation energy. However, the electron detection efficiencies f_s and f_d would be considerably different because of different kinetic energies of each photoelectron and the different number of electrons in the two processes.

The ion-ion coincidence rate (C_{II}) was obtained by integrating the PIPICO peaks. The ion and electron detec-

tion efficiencies $f_i(=0.050)$ and $f_s(=0.11)$ were determined from Eqs. (2), (3), and (4) at an excitation energy of 37 eV where only the single photoionization occurs. The low ion detection efficiency of 0.05 is due to an aging effect caused by using the same detector for a long period.

As described in Sec. III B, the ratio of double photoionization to single photoionization (N_d/N_s) and the dissociation ratio ($\xi_d+\zeta_d$) of NO^{2+} are strongly dependent on the ratio f_d/f_s of the electron detection efficiencies [see Eqs. (6), (7), and (8)]. In order to evaluate the ratio f_d/f_s, the ratio N_d/N_s was measured for Ar in the region from the double-photoionization threshold to 100 eV. The result was quite different from those previously reported [30]. The ratio of the present value $[Ar^{2+}:Ar^+]_p$ to that of reported $[Ar^{2+}:Ar^+]_r$ was increased continuously from the double-photoionization threshold to about 80 eV and reached an asymptotic value of about 2.5 above 80 eV. This discrepancy can most probably be ascribed to the energy-dependent character of the ratio f_d/f_s. At 60 eV, for example, the kinetic energy of photoelectrons ejected from the ground state of NO^+ is of the order of 50 eV, whereas that from the ground state of NO^{2+} is about 20 eV. These more energetic photoelectrons produced by single photoionization would be more easily discriminated in the TOF mass spectrometer than those produced by double photoionization. Because the total electron signals were used as the start pulses of the TAC, this discrimination effect results in an underestimation of the ions produced in single photoionization. In contrast, the different number of ejected electrons in single and double photoionization causes an overestimation of the ions produced in double photoionization because the probability of forming one output pulse in the electron detector is higher for two electrons hitting in sequence than for one electron [7].

The apparent ion branching ratios directly obtained from the mass spectrometer are shown in Fig. 2 and compared with those reported by Iida *et al.* [4]. Apparently NO^{2+}, N^+, and O^+ ions produced in double photoionization are overestimated and NO^+ is underestimated at higher photon energies. By assuming that the data obtained by the dipole (electron, electron plus ion) method [4] is not affected by the discrimination effect mentioned above, the ratio f_d/f_s in the present TOF mass spectrometer was estimated from the following equation:

$$\frac{f_d}{f_s}=\frac{R_A(AB^{2+}+A^{2+}+B^{2+})}{R_A(AB^+)}\frac{R_B(AB^+)}{R_B(AB^{2+})}\ , \tag{6}$$

where R_A is the apparent ion branching ratio obtained in the present study and R_B is the one reported in Ref. [4].

B. Determination of single- and double-photoionization cross sections

The single- and double-photoionization cross sections σ^+ and σ^{2+} were obtained as a function of excitation energy. When the precursor NO^{2+} is partially dissociative above 41.0 eV, the ratio of double to single photoionization is given from Eqs. (2) and (5) by

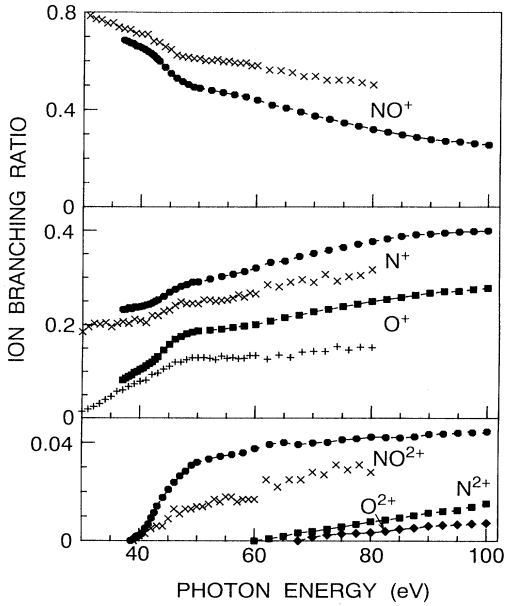

FIG. 2. Ion branching ratios directly obtained from the mass spectra as a function of photon energy. ● and ■, present data; × and +, from Ref. [4].

$$\frac{N_d}{N_s}=\frac{1}{f_i I\xi_d/C_{II}-(1+\xi_d)}\ . \tag{7}$$

The ion branching ratio $R_A(AB^{2+}+A^{2+}+B^{2+})$ for the doubly charged AB^{2+}, A^{2+}, and B^{2+} ions obtained directly from the mass spectrum is given by

$$R_A(AB^{2+}+A^{2+}+B^{2+})=\frac{f_d(1-\xi_d)N_d}{f_sN_s+f_d(1+\xi_d)N_d}\ , \tag{8}$$

where the denominator represents C_{EI}/f_i [see Eq. (4)].

At the photon energies where the NO^{2+} ion is nondissociative (i.e., $38.5<h\nu<41.0$ eV), the ratio of double to single photoionization is given from Eq. (8) by

$$\frac{N_d}{N_s}=\frac{f_sR_A(AB^{2+})}{f_d[1-R_A(AB^{2+})]}\ . \tag{9}$$

At the photon energies where the NO^{2+} ions are partially dissociative, N_d/N_s and ξ_d were calculated from Eqs. (7) and (8). These rates (N_s and N_d) were converted to the cross sections of the single and double photoionization by using the total photoionization cross sections reported by Iida *et al.* as a function of excitation energy [4].

C. Determination of the ion branching ratios and the partial cross sections for the fragmentation of NO^+ and NO^{2+}

It is clear that the apparent ion branching ratio $R_A(A^+)$ for the A^+ fragment ion obtained directly from the mass spectrum at higher photon energies is the sum of those related to single (A_s^+) and double (A_d^+) photoionization. That is,

$$R_A(A^+)=R_A(A_s^+)+R_A(A_d^+)\ . \tag{10}$$

The two terms on the right-hand side in Eq. (10) are still apparent ion branching ratios and can be related to the inherent ion branching ratios $R(A_s^+)$ and $R(A_d^+)$ for the A_s^+ and A_d^+ ions, respectively, resulting from the precursors NO^+ and NO^{2+}, by the following equations:

$$R_A(A_s^+)=\frac{f_sN_s}{f_sN_s+f_d(1+\xi_d)N_d}R(A_s^+)\ , \tag{11}$$

$$R_A(A_d^+)=\frac{f_dN_d}{f_sN_s+f_d(1+\xi_d)N_d}R(A_d^+)\ . \tag{12}$$

Because the dissociation channel of NO^{2+} is only N^++O^+, $R(A_d^+)$ equals ξ_d. Thus $R_A(A_d^+)$ is determined directly from Eq. (12). $R_A(A_s^+)$ is determined from Eq. (10) and by substituting the result into Eq. (11) we can finally determine $R(A_s^+)$. That is,

$$R(A_s)=R_A(A^+)[1+(1+\xi_d)f_rx]-f_rx\xi_d\ , \tag{13}$$

where $f_r=f_d/f_s$ and $x=N_d/N_s$.

IV. RESULTS AND DISCUSSION

A. Single- and double-photoionization cross sections

The ratio of double to single photoionization determined by the method described in Sec. III B is shown in Fig. 3 and listed in Table I. The absolute cross sections for the single and double photoionization shown in Fig. 4 (Table I) were obtained from the total cross sections σ_t [4] assuming that $\sigma_t=\sigma^++\sigma^{2+}$. It should be emphasized that the double-photoionization cross sections reported in Figs. 3 and 4 include both the dissociative and nondissociative processes of the precursor NO^{2+}.

The appearance potential of NO^{2+} (38.5±0.1 eV) was found to be in excellent agreement with the value of 38.6±0.1 eV very recently reported by Pettersson *et al.* [2]. Two other independent experiments also give the same values of 38.6±0.1 [15] and 38.6±0.3 eV [14] as the appearance energy of NO^{2+}. The vertical energies of the $A\ ^2\Pi$ and $B\ ^2\Sigma^+$ states are reported, respectively, to be 40.0 and 42.5±0.5 eV by the PIFCO method [15,16]. The corresponding energies observed by Auger spectroscopy [2], which do not contain any structures due to autoionization, in contrast to the results previously reported by Auger spectroscopy [8], are 40.1 (O 1*s*) or 40.2 (N 1*s*) eV for the $A\ ^2\Pi$ state and 43.4 (O 1*s*) or 43.3 (N 1*s*) eV for the $B\ ^2\Sigma^+$ state. The higher value (43.3 eV) of the $B\ ^2\Sigma^+$ state is in good agreement with the vertical energy gap of the $X\ ^2\Sigma^+$ and $B\ ^2\Sigma^+$ states obtained by translational energy spectroscopy [10–12].

There are no obvious breaks in the ratio σ^{2+}/σ^+ and the cross-section σ^{2+} curves at the excitation energies

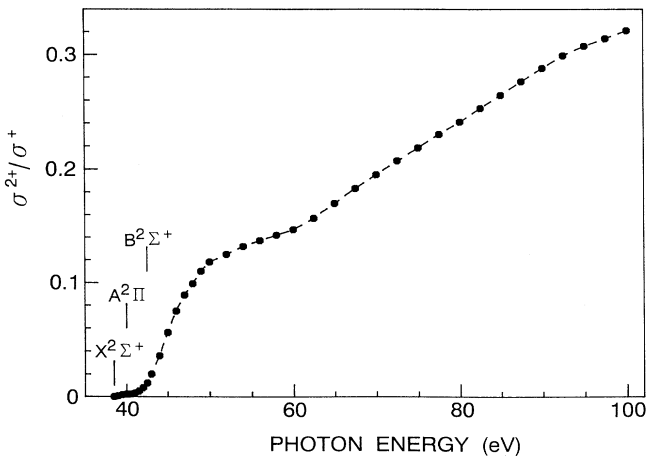

FIG. 3. Double-photoionization cross section (σ^{2+}) relative to single-photoionization cross section (σ^+) of NO. The $X\ ^2\Sigma^+$, $A\ ^2\Pi$, and $B\ ^2\Sigma^+$ states of NO^{2+} are from Refs. [15,16].

TABLE I. Cross sections for the single and double photoionization of NO (in Mb) and their ratio.

Photon energy (eV)	σ^+	σ^{2+}	σ^{2+}/σ^+
37.0	15.29		
37.5	15.16		
38.0	15.01		
38.5	14.77	0	0
39.0	14.51	0.010	0.0007
39.5	14.17	0.026	0.0018
40.0	13.82	0.030	0.0022
40.5	13.71	0.034	0.0025
41.0	13.58	0.045	0.0033
41.5	13.46	0.067	0.0050
42.0	13.34	0.11	0.0080
42.5	13.17	0.16	0.012
43.0	12.93	0.26	0.020
44.0	12.60	0.45	0.036
45.0	12.04	0.67	0.056
46.0	11.63	0.87	0.075
47.0	11.29	1.00	0.089
48.0	10.91	1.08	0.099
49.0	10.55	1.16	0.110
50.0	10.09	1.19	0.118
52.0	9.24	1.15	0.125
54.0	8.54	1.13	0.132
56.0	7.95	1.09	0.137
58.0	7.23	1.03	0.142
60.0	6.66	0.98	0.147
62.5	6.17	0.97	0.157
65.0	5.69	0.97	0.170
67.5	5.28	0.97	0.183
70.0	4.88	0.95	0.195
72.5	4.37	0.91	0.207
75.0	4.13	0.90	0.218
77.5	3.87	0.89	0.230
80.0	3.49	0.84	0.241
82.5	3.17	0.80	0.253
85.0	2.88	0.76	0.265
87.5	2.67	0.74	0.277
90.0	2.50	0.72	0.288
92.5	2.35	0.70	0.299
95.0	2.23	0.69	0.308
97.5	2.09	0.66	0.314
100.0	1.99	0.64	0.321

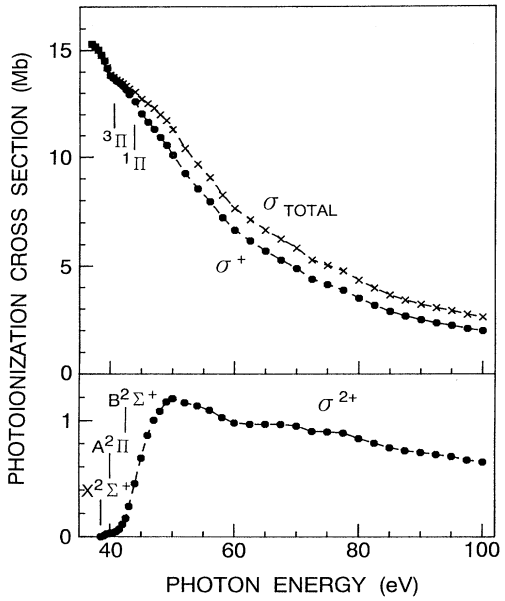

FIG. 4. Cross sections for single (σ^+) and double (σ^{2+}) photoionization of NO. The total cross section (σ_{total}) is from Ref. [4]. The $^{3,1}\Pi$ states of NO^+ are from Ref. [37]. The $X\,^2\Sigma^+$, $A\,^2\Pi$, and $B\,^2\Sigma^+$ states of NO^{2+} are from Refs. [15,16].

corresponding to the $A\,^2\Pi$ and $B\,^2\Sigma^+$ states. Even if the quartet states of NO^{2+} are taken into consideration, only the $A\,^2\Pi$ and $B\,^2\Sigma^+$ excited states exist in the region of 40–44 eV, from theoretical calculations [25]. The absence of obvious breaks (Figs. 3 and 4) in this region suggests that the molecular and dissociative NO^{2+} ions are produced from autoionizing Rydberg states densely existing in this region.

The region of 43.5–47.5 eV is a Franck-Condon gap of NO^{2+}, where no doublet states exist [2]. In this region, the ratio σ^{2+}/σ^+ (Fig. 3) and the cross-section σ^{2+} (Fig. 4) increase rather steeply with energy. This is again due to a contribution of autoionizing Rydberg states in the production of the molecular and dissociative NO^{2+} ions. The large number of closely spaced ionic states of NO^{2+} in the region of 47.5–57.5 eV will have a correspondingly large number of manifolds of Rydberg states converging to them, which will autoionize by interaction with the underlying ionization continua of the $X\,^2\Sigma^+$, $A\,^2\Pi$, and $B\,^2\Sigma^+$ states. The closely spaced ionic states of NO^{2+} just mentioned have been reported in the region of 47.5–57.5 eV by recent *ab initio* calculations [2] and contribute to the increase in the ratio σ^{2+}/σ^+ in this region. Higher-lying electronic states of NO^{2+}, which contribute to the increase in the ratio σ^{2+}/σ^+ above 57.5 eV, can be found in the work reported by Moddeman *et al.* [8].

The presently obtained ratio σ^{2+}/σ^+ for NO is in close agreement with that for CS_2 [31] and OCS [5] and is considerably higher, an order of magnitude or more, than the reported values for SO_2, CO_2, and CH_4 [32–34]. However, the possibility of underestimation in the ratio σ^{2+}/σ^+ for the latter molecules has been pointed out [7].

B. Ion branching ratios and the partial cross sections for the fragmentation of NO^+

The ion branching ratios for the precursor NO^+ obtained by the method mentioned above, thus separately determined from those for NO^{2+}, are shown in Fig. 5 (Table II). The remarkable changes in the ion branching ratios shown in Fig. 5 are found for the NO^+ and O^+ ions compared with those obtained directly from the mass spectra (Fig. 2).

The ion branching ratio of NO^+ shows an interesting behavior in the region 37–50 eV: the ratio first decreases gradually in the region 37–42.5 eV and then increases. This increase in the ion branching ratio for NO^+ indicates the presence of the bound-type Rydberg states of

TABLE II. Ion branching ratios and the partial cross sections for the fragmentation of NO^+.

Photon energy	Branching ratio			Cross section (Mb)		
(eV)	N^+	O^+	NO^+	N^+	O^+	NO^+
37.0	0.232	0.082	0.686	3.55	1.25	10.49
37.5	0.233	0.086	0.681	3.53	1.30	10.33
38.0	0.236	0.090	0.674	3.55	1.34	10.12
38.5	0.235	0.093	0.673	3.47	1.37	9.94
39.0	0.239	0.099	0.663	3.46	1.43	9.62
39.5	0.238	0.101	0.661	3.37	1.43	9.37
40.0	0.239	0.105	0.655	3.31	1.46	9.06
40.5	0.241	0.109	0.650	3.31	1.49	8.91
41.0	0.244	0.113	0.643	3.31	1.54	8.73
41.5	0.244	0.116	0.640	3.29	1.56	8.62
42.0	0.245	0.116	0.639	3.27	1.55	8.52
42.5	0.246	0.117	0.638	3.23	1.53	8.40
43.0	0.241	0.111	0.648	3.12	1.43	8.39
44.0	0.233	0.100	0.668	2.93	1.26	8.41
45.0	0.223	0.083	0.694	2.68	1.00	8.35
46.0	0.211	0.067	0.721	2.46	0.78	8.39
47.0	0.206	0.053	0.742	2.32	0.59	8.37
48.0	0.201	0.046	0.753	2.19	0.50	8.21
49.0	0.199	0.034	0.767	2.10	0.36	8.09
50.0	0.192	0.026	0.782	1.94	0.27	7.89
52.0	0.197	0.019	0.784	1.82	0.18	7.24
54.0	0.200	0.014	0.786	1.71	0.12	6.72
56.0	0.204	0.013	0.783	1.62	0.10	6.23
58.0	0.210	0.011	0.779	1.52	0.08	5.63
60.0	0.221	0.011	0.768	1.47	0.07	5.12
62.5	0.225	0.013	0.762	1.39	0.08	4.70
65.0	0.233	0.011	0.756	1.33	0.06	4.31
67.5	0.243	0.004	0.753	1.28	0.02	3.98
70.0	0.251	0.006	0.743	1.23	0.03	3.62
72.5	0.259	0.004	0.737	1.13	0.02	3.22
75.0	0.268	0.006	0.726	1.10	0.03	3.00
77.5	0.278	0.005	0.717	1.08	0.02	2.78
80.0	0.287	0.007	0.705	1.00	0.03	2.46
82.5	0.296	0.005	0.699	0.94	0.02	2.22
85.0	0.304	0.004	0.692	0.88	0.01	1.99
87.5	0.310	0.005	0.685	0.83	0.01	1.82
90.0	0.314	0.009	0.677	0.78	0.02	1.69
92.5	0.316	0.008	0.676	0.74	0.02	1.59
95.0	0.320	0.002	0.678	0.71	0.01	1.51
97.5	0.323	0.007	0.670	0.67	0.02	1.40
100.0	0.327	0.011	0.663	0.65	0.02	1.32

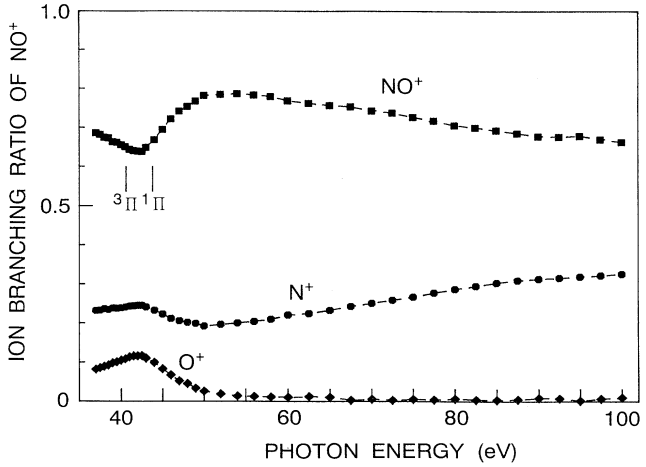

FIG. 5. Ion branching ratios of single photoionization of NO. The $^{3,1}\Pi$ states of NO^+ are from Ref. [37].

the neutral (double Rydberg) and singly charged ion converging to the electronic states of NO^{2+} lying above 42.5 eV. Another possibility is that the Rydberg states autoionize to the low-lying bound electronic states [4] ($X\,^1\Sigma^+$, $a\,^3\Sigma^+$, $b\,^3\Pi$, $w\,^3\Delta$, $b'\,^3\Sigma^+$, $A'\,^1\Sigma^-$, $A\,^1\Pi$, and $W\,^1\Delta$) of NO^+. In the region (42.5–50 eV) where the ion branching ratio for NO^+ increases, those for N^+ and O^+ decrease. However, the decrease in N^+ is more gradual than that in O^+, and furthermore the ion branching ratio for N^+ increases above 50 eV, which is in sharp contrast to that for O^+. This suggests that the repulsive electron-

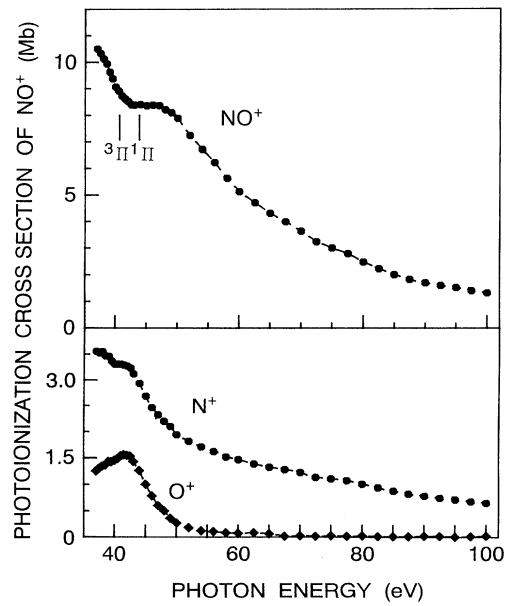

FIG. 6. Partial photoionization cross sections for the ions produced from the precursor NO^+. The $^{3,1}\Pi$ states of NO^+ are from Ref. [37].

ic states of NO^+ lying above 42.5 eV dissociate only to N^+. The ion branching ratio of NO^+ decreases gradually above 50 eV as a reaction to the increase of N^+.

The partial cross sections for the respective channels of NO^+ are shown in Fig. 6 (see Table II). The increase in the ion branching ratio for NO^+ in the region 42.5–50 eV causes a shoulder around 47 eV in the partial cross section for NO^+.

C. Ion branching ratios and the partial cross sections for the fragmentation of NO^{2+}

The ion branching ratios for the precursor NO^{2+} separately determined from those for NO^+ are shown in Fig. 7 (Table III). The abundance of the metastable NO^{2+} increases to 15% at 60 eV, in contrast to the value of about 4% in Fig. 2, thus indicating the necessity of determining the ion branching ratios for single and double photoionization separately. The partial cross sections for the

TABLE III. Ion branching ratios of NO^{2+}.

Photon energy (eV)	$N^+ + O^+$	NO^{2+}	N^{2+}	O^{2+}
38.5		0		
39.0		1.000		
39.5		1.000		
40.0		1.000		
40.5		1.000		
41.0	0	1.000		
41.5	0.285	0.715		
42.0	0.438	0.562		
42.5	0.563	0.437		
43.0	0.676	0.324		
44.0	0.773	0.227		
45.0	0.816	0.184		
46.0	0.834	0.166		
47.0	0.839	0.161		
48.0	0.841	0.159		
49.0	0.841	0.159		
50.0	0.842	0.158		
52.0	0.841	0.159		
54.0	0.842	0.158		
56.0	0.842	0.158		
58.0	0.842	0.158		
60.0	0.838	0.162	0	
62.5	0.833	0.163	0.004	
65.0	0.833	0.159	0.008	
67.5	0.837	0.150	0.013	0
70.0	0.832	0.148	0.015	0.006
72.5	0.830	0.144	0.017	0.009
75.0	0.825	0.144	0.020	0.010
77.5	0.824	0.142	0.023	0.011
80.0	0.821	0.141	0.027	0.011
82.5	0.822	0.138	0.028	0.013
85.0	0.820	0.134	0.030	0.015
87.5	0.818	0.133	0.033	0.017
90.0	0.812	0.134	0.036	0.019
92.5	0.811	0.132	0.037	0.020
95.0	0.811	0.132	0.038	0.020
97.5	0.807	0.131	0.042	0.021
100.0	0.802	0.131	0.045	0.022

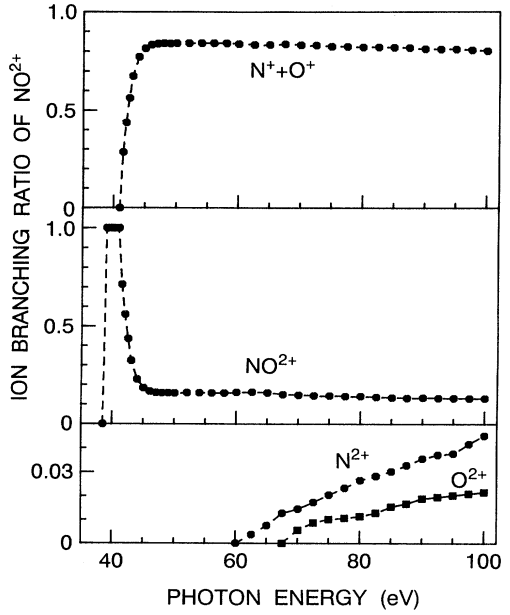

FIG. 7. Ion branching ratios of double photoionization of NO.

respective channels are shown in Fig. 8 and listed in Table IV.

Only the metastable NO^{2+} ions are produced in double photoionization in the 38.5–41.0-eV region. The dissociation threshold of NO^{2+} is found to be 41.0±0.3 eV, which is in close agreement with 40.3 eV reported by Brehm and De Frênes [19]. This means that the $X\,^2\Sigma^+$ state and a lower part of the $A\,^2\Pi$ state are bound. According to theoretical calculations reported by Pettersson

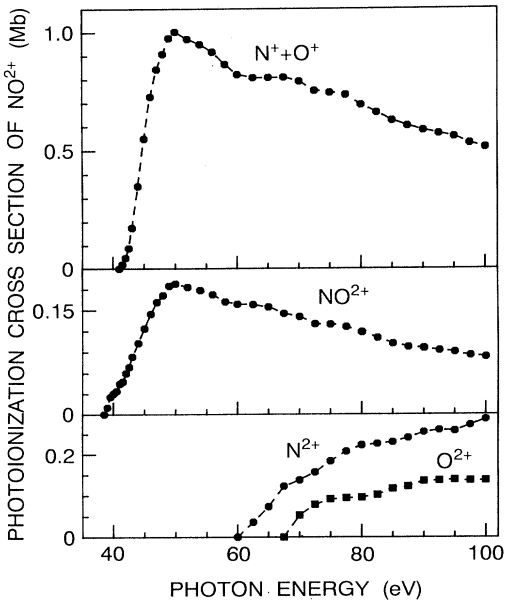

FIG. 8. Partial photoionization cross sections for the ions produced from the precursor NO^{2+}.

et al. [27], the vibrational levels with $v \geq 7$ of the $A\,^2\Pi$ state are dissociative in a μsec time scale. From the calculations, the $v=7$ level lies 2.45 eV above the $v=0$ level of the $X\,^2\Sigma^+$ state. The appearance potential of NO^{2+} (38.5 eV in the present work) plus this energy (2.45 eV) gives 40.95 eV, which is in excellent agreement with the presently observed value for ion-pair production ($N^+ + O^+$).

Above 41.0 eV, where the dissociative states of NO^{2+} are energetically accessible, the ion branching ratio of molecular NO^{2+} ion decreases rapidly and reaches a constant value of 15% above about 45 eV. This indicates that bound or partially bound electronic states of NO^{2+} exist at the higher-energy region. Another possibility for the production of stable NO^{2+} is that the superexcited NO^{**} and NO^{+*} to Rydberg states converging to high-lying electronic states of NO^{2+} autoionize to the low-

TABLE IV. Partial cross sections for the fragmentation of NO^{2+} (in Mb).

Photon energy (eV)	$N^+ + O^+$	NO^{2+}	N^{2+}	O^{2+}
38.5		0		
39.0		0.010		
39.5		0.026		
40.0		0.030		
40.5		0.034		
41.0	0	0.045		
41.5	0.019	0.048		
42.0	0.047	0.060		
42.5	0.089	0.069		
43.0	0.175	0.084		
44.0	0.350	0.103		
45.0	0.550	0.124		
46.0	0.727	0.145		
47.0	0.843	0.161		
48.0	0.908	0.171		
49.0	0.976	0.185		
50.0	1.003	0.188		
52.0	0.972	0.183		
54.0	0.949	0.179		
56.0	0.917	0.172		
58.0	0.864	0.162		
60.0	0.821	0.158	0	
62.5	0.807	0.158	0.004	
65.0	0.807	0.154	0.007	
67.5	0.809	0.145	0.012	0
70.0	0.792	0.140	0.014	0.005
72.5	0.752	0.130	0.016	0.008
75.0	0.744	0.130	0.018	0.009
77.5	0.734	0.126	0.021	0.010
80.0	0.691	0.119	0.022	0.010
82.5	0.659	0.110	0.023	0.010
85.0	0.625	0.102	0.023	0.012
87.5	0.603	0.098	0.024	0.012
90.0	0.584	0.096	0.026	0.014
92.5	0.570	0.093	0.026	0.014
95.0	0.557	0.090	0.026	0.014
97.5	0.529	0.086	0.027	0.014
100.0	0.512	0.083	0.029	0.014

lying bound state of NO^{2+} such as $X\,^2\Sigma^+$, $A\,^2\Pi$, and $B\,^2\Sigma^+$.

The appearance potentials of N^{2+} and O^{2+} are found to be 60.0±1 and 67.5±1 eV, respectively. Corresponding values of 56.0±0.2 and 61.6±0.15 eV have been reported by Hierl and Franklin [35] and 57.6±1.0 and 62.2±1.0 eV by Newton and Sciamanna [36]. Since the ion branching ratios of N^{2+} and O^{2+} are less than 0.5% in the 60–100-eV region, the production of the doubly charged fragment ions is a very minor process in double photoionization.

D. Dissociation ratios of NO^+ and NO^{2+}

The separate determination of the ion branching ratios for the precursors NO^+ and NO^{2+} was used to obtain the dissociation ratios (ξ_s and $\xi_d+\zeta_d$) of the singly and doubly charged precursors, and the results are shown in Fig. 9. It is interesting to note that the dissociation ratio of NO^{2+} reaches an asymptotic value very close to 0.85 at about 46 eV. This trend is very similar to the result obtained for OCS^{2+} [7]. The ground state of NO^{2+}, $X\,^2\Sigma^+$, and the first ($A\,^2\Pi$) and the second excited ($B\,^2\Sigma^+$) states of NO^{2+} are known to be quasibound [2,15,16,26]. If these bound states are the only source for the stable NO^{2+}, the dissociation ratio should increase at higher photon energies. The observation of the asymptotic value suggests the presence of bound electronic states at higher photon energies and/or autoionization of high-lying Rydberg states to the low-lying bound states of NO^{2+}, as discussed in Sec. IV C.

Conversely, the fact that the dissociation ratio of NO^+ decreases above 42.5 eV means that the Rydberg states converging to the low-lying electronic states of NO^{2+} are nondissociative and/or autoionizing to the low-lying bound states of NO^+ and produce the stable NO^+ ions. Above about 56 eV, the dissociation ratio of NO^+ increases. However, the nondissociative process is still dominant even at higher photon energies. This strongly suggests that the majority of the high-lying electronic states of NO^+ is nondissociative and/or the contribution of autoionizing Rydberg states to the low-lying bound states of NO^+.

V. CONCLUSIONS

By developing a method to analyze mass and PIPICO spectra, the cross sections for the single and double photoionization have been successfully determined for NO,

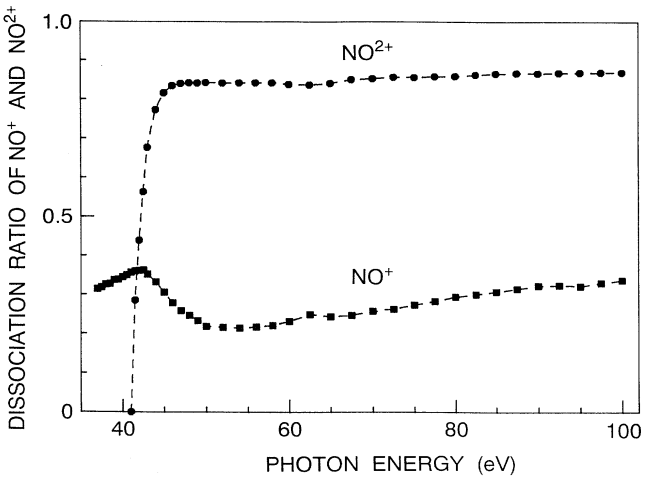

FIG. 9. Dissociation ratios of the precursors of NO^+ and NO^{2+}.

in which both dissociative and nondissociative processes take place concomitantly. The method employed in the present study also makes it possible to determine the ion branching ratios and the partial cross sections for the ions produced from the precursor NO^+ separately from those of NO^{2+}. It is found that in the single photoionization the production of the stable NO^+ ions is a dominant process throughout the energy region examined, whereas in the double photoionization the dissociation becomes a dominant process above about 5 eV from the double-photoionization threshold. For the production of the stable NO^+ and NO^{2+} ions at higher photon energies, it is pointed out that the bound-type electronic states of NO^+ and NO^{2+} do exist and/or the Rydberg states play an important role through autoionization. The charge-localized dissociation of NO^{2+} leading to the production of N^{2+} and O^{2+} is also observed as a very minor process in the region of the inner-valence double photoionization.

ACKNOWLEDGMENTS

Sincere gratitude is extended to the UVSOR personnel for their beneficial assistance during the experiments. This work was supported by the UVSOR Joint Research Program of the Institute for Molecular Science and in part by Grants-in-Aid for Scientific Research No. 04640455 from Japan's Ministry of Education, Science and Culture.

[1] V. Krishnamurthi, K. Nagesha, V. R. Marathe, and D. Mathur, Phys. Rev. A **44**, 5460 (1991), and references therein.

[2] L. G. M. Pettersson, L. Karlsson, M. P. Keane, A. Naves de Brito, N. Correia, M. Larsson, L. Broström, S. Mannervik, and S. Svensson, J. Chem. Phys. **96**, 4884 (1992), and references therein.

[3] J. A. R. Samson, T. Masuoka, and P. N. Pareek, J. Chem. Phys. **83**, 5531 (1985).

[4] Y. Iida, F. Carnovale, S. Daviel, and C. E. Brion, Chem. Phys. **105**, 211 (1986).

[5] F. H. Dorman and J. D. Morrison, J. Chem. Phys. **35**, 575 (1961).

[6] Y. B. Kim, K. Stephan, E. Märk, and T. D. Märk, J. Chem. Phys. **74**, 6771 (1981).

[7] T. Masuoka and H. Doi, Phys. Rev. A **47**, 278 (1993).

[8] W. E. Moddeman, T. A. Carlson, M. O. Krause, B. P. Pullen, W. E. Bull, and G. K. Schweitzer, J. Chem. Phys. **55**, 2317 (1971).
[9] A. O'Keefe, A. J. Illies, J. R. Gilbert, and M. T. Bowers, Chem. Phys. **82**, 471 (1983).
[10] P. Jonathan, R. K. Boyd, A. G. Brenton, and J. H. Beynon, Int. J. Mass Spectrom. Ion Proc. **68**, 91 (1986).
[11] P. Jonathan, Z. Herman, M. Hamdan, and A. G. Brenton, Chem. Phys. Lett. **141**, 511 (1987).
[12] M. Hamdan and A. G. Brenton, Chem. Phys. Lett. **155**, 321 (1989).
[13] J. Appell, J. Durup, F. C. Fehsenfeld, and P. Fournier, J. Phys. B **6**, 197 (1973).
[14] P. G. Fournier and R. E. March, Chem. Phys. Lett. **137**, 596 (1987).
[15] M. J. Besnard, L. Hellner, Y. Malinovich, and G. Dujardin, J. Chem. Phys. **85**, 1316 (1986).
[16] M. J. Besnard, L. Hellner, and G. Dujardin, J. Chem. Phys. **89**, 6554 (1988).
[17] J. H. Beynon, R. M. Caprioli, and J. W. Richardson, J. Am. Chem. Soc. **93**, 1852 (1971).
[18] D. M. Curtis and J. H. D. Eland, Int. J. Mass Spectrom. Ion Proc. **63**, 241 (1985).
[19] B. Brehm and G. de Frênes, Int. J. Mass Spectrom. Ion Phys. **26**, 251 (1978).
[20] J. M. Curtis and R. K. Boyd, J. Chem. Phys. **81**, 2991 (1984).
[21] D. Cossart, M. Bonneau, and J. M. Robbe, J. Mol. Spectrosc. **125**, 413 (1987).
[22] D. Cossart and C. Cossart-Magos, J. Mol. Spectrosc. **147**, 471 (1991).
[23] A. C. Hurley, J. Mol. Spectrosc. **9**, 18 (1962).
[24] P. W. Thulstrup, E. W. Thulstrup, A. Andersen, and Y. Öhrn, J. Chem. Phys. **60**, 3975 (1974).
[25] R. W. Wetmore and R. K. Boyd, J. Phys. Chem. **90**, 6091 (1986).
[26] D. L. Cooper, Chem. Phys. Lett. **132**, 377 (1986).
[27] L. G. M. Pettersson, P. E. M. Siegbahn, L. Broström, S. Mannervik, and M. Larsson, Chem. Phys. Lett. **191**, 279 (1992).
[28] T. Masuoka and I. Koyano, J. Chem. Phys. **95**, 909 (1991).
[29] T. Masuoka, T. Horigome, and I. Koyano, Rev. Sci. Instrum. **60**, 2179 (1989).
[30] D. M. P. Holland, K. Codling, J. B. West, and G. V. Marr, J. Phys. B **12**, 2465 (1979).
[31] P. Lablanquie, I. Nenner, P. Millie, P. Morin, J. H. D. Eland, M. J. Hubin-Franskin, and J. Delwiche, J. Chem. Phys. **82**, 2951 (1985).
[32] G. Dujardin, S. Leach, O. Dutuit, P. M. Guyon, and M. Richard-Viard, Chem. Phys. **88**, 339 (1984).
[33] G. Dujardin, D. Winkoun, and S. Leach, Phys. Rev. A **31**, 3027 (1985).
[34] G. Dujardin and D. Winkoun, J. Chem. Phys. **83**, 6222 (1985).
[35] P. M. Hierl and J. L. Franklin, J. Chem. Phys. **47**, 3154 (1967).
[36] A. S. Newton and A. F. Sciamanna, J. Chem. Phys. **50**, 4868 (1969).
[37] K. Siegbahn, C. Nordling, G. Johansson, J. Hedman, P. F. Heden, K. Hamrin, U. Gelius, T. Bergmark, L. O. Werme, R. Manne, and Y. Bare, *ESCA Applied to Free Molecules* (North-Holland, Amsterdam, 1971).